2023 IEEE 66th International Midwest Symposium on Circuits and Systems (MWSCAS)
Phoenix, Arizona, USA, August 6-9, 2023

Pulsed ToF LiDAR-based Depth Imaging: SPAD Circuit Considerations and Simulation Study

Utku Noyan[1], Sheung Lu[1], Abdullah Al-Shabili[2], Marc Dandin[3], Stanley H. Chan[2], and Pamela Abshire[1]

2023 IEEE 66th International Midwest Symposium on Circuits and Systems (MWSCAS) | 979-8-3503-0210-3/23/$31.00 ©2023 IEEE | DOI: 10.1109/MWSCAS57524.2023.10405999

***Abstract*—Pulsed Time-of-Flight (ToF) LiDAR is a crucial technology for acquiring depth information in various applications, including autonomous vehicles, robotics, and 3D mapping. Single-Photon Avalanche Diodes (SPADs) are widely employed as detectors in these systems due to their fast response and high sensitivity. This paper investigates pulsed ToF LiDAR-based depth imaging to clarify the hardware design considerations that affect depth estimation accuracy. We present a simulation study that investigates the performance of SPAD-based LiDAR systems under various conditions, offering insights into the design of SPAD circuits for improved depth imaging performance. We find that, as expected, accuracy and depth resolution depend strongly on the fill factor, with accuracy decreasing as the fill factor drops, gradually at first and then more steeply for fill characteristics of less than 50%. Lastly, we discuss the outcomes of our simulations and suggest directions for future research in this area.**

***Index Terms*—Depth imaging, Pulsed Time-of-Flight (ToF) LiDAR, Single-Photon Avalanche Diodes (SPADs), Autonomous vehicles Circuit considerations**

I. Introduction

Depth imaging plays a pivotal role in various fields, including robotics, autonomous vehicles [1], and 3D mapping. Among the depth imaging technologies, Pulsed Time-of-Flight (ToF) LiDAR systems have gained substantial recognition due to their ability to deliver accurate, high-resolution depth information. These systems predominantly employ Single-Photon Avalanche Diodes (SPADs) [2], recognized for their rapid response and high sensitivity stemming from the avalanche effect. SPAD circuit considerations are therefore critical in determining the accuracy and performance of depth estimation [3]. Despite the importance of these considerations, the tradeoffs related to the design and performance of SPAD circuits in LiDAR systems remain under-explored. One notable application of LiDAR systems with optimized fill factors and sensitivity is autonomous driving, where accurate, reliable, and timely depth sensing is essential for safe navigation and obstacle detection [4]. This paper attempts to bridge this gap by investigating the tradeoffs in pulsed ToF LiDAR-based depth imaging, focusing on SPAD hardware factors. This simulation study offers new insights into the influence of hardware design factors on system performance, with a view to optimizing depth, accuracy, and efficiency.

[1]Utku Noyan, Sheung Lu, and Pamela Abshire are with the Department of Electrical and Computer Engineering and Institute of System Research at the University of Maryland, College Park, MD, USA. e-mail: (pabshire@umd.edu).
[2]Abdullah Al-Shabili and Stanley H. Chan are with the Department of Electrical and Computer Engineering at Purdue University, West Lafayette, IN, USA.
[3]Marc Dandin is with the Department of Electrical and Computer Engineering at Carnegie Mellon University, Pittsburgh, PA.
This work was supported by COGNISENSE, one of seven centers in JUMP 2.0, a Semiconductor Research Corporation (SRC) program sponsored by DARPA.

The paper is organized as follows: Section II briefly introduces pulsed ToF LiDAR-based depth imaging. Section III discusses these systems' circuit considerations for SPADs. Section IV presents the simulation study methodology and its assumptions. Section V discusses the results obtained from the simulations and their implications. Finally, Section VI concludes the paper and suggests future research directions.

II. Pulsed ToF LIDAR-based Depth Imaging

Pulsed ToF LIDAR systems, as illustrated in Figure 1, utilize short laser pulses to illuminate a scene and measure the time required for light to travel from the source to the target and back to the detector - the time of flight (ToF). These short pulses are beneficial as they allow for higher-resolution measurements and are less likely to be affected by ambient light. The time-of-flight is then used to calculate the distance between the LIDAR system and the target, providing precise depth information.

A typical pulsed ToF LIDAR system, as illustrated in Figure 2, comprises a light source, a detector array, a timing circuit, and signal processing components. The light source emits short laser pulses, and the detector, typically a SPAD array, captures the photons reflected from the scene. SPADs are particularly favored in this setting due to their fast response time and high sensitivity. The timing circuit measures the time-of-flight for each detected photon, while the signal processing components transform the raw data into depth information to construct a detailed depth map of the scene.

The relationship between time-of-flight and distance is given by:

$$d = \frac{c \times t}{2} \tag{1}$$

where d is the distance to the target, c is the speed of light, and t is the time of flight. Pulsed ToF LIDAR systems offer several advantages over other depth imaging technologies such as structured light and stereo vision. They are less affected by ambient lighting conditions, can work at longer ranges, and provide higher depth resolution [1]. Performance can be degraded by atmospheric conditions such as fog, as these can affect the transmission of the LIDAR light pulse. This point is particularly relevant when considering real-world application scenarios. Design of an efficient pulsed ToF LIDAR system requires careful consideration of various factors, including

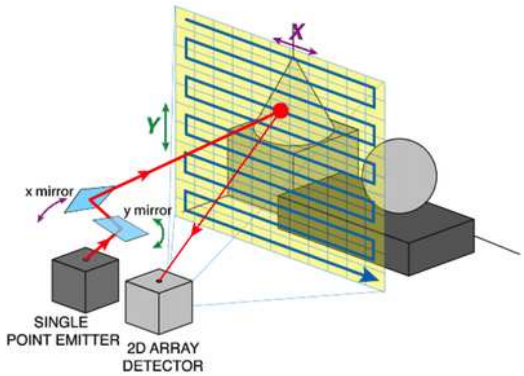

Fig. 1: TOF-LIDAR illumination schemes: 2D raster scan with single spot and a 2D array detector. Adapted from SPADs and SiPMs Arrays for Long-Range High-Speed Light Detection and Ranging (LIDAR) by Villa et al. [5] (available from [6], used under CC BY 4.0.

the choice of detectors, light sources, and signal processing techniques. In particular, the performance of SPAD-based detectors significantly impacts the overall depth estimation accuracy and system performance.

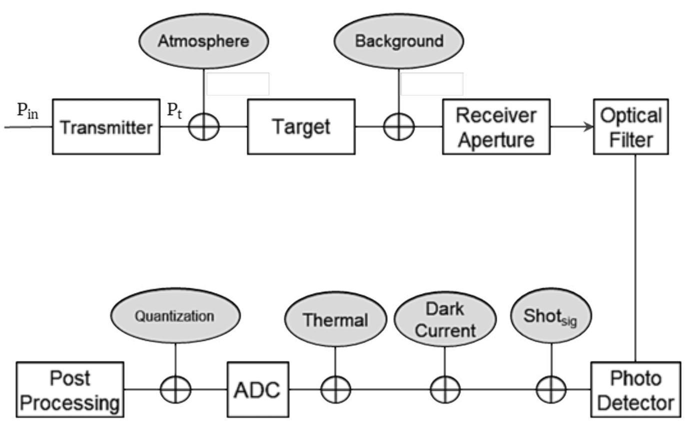

Fig. 2: Communication Channel Model of Pulsed ToF LIDAR Front End including Circuit Considerations

III. SPAD Circuit Considerations

Single-Photon Avalanche Diodes (SPADs) are P-N junctions operated in avalanche with high sensitivity, allowing them to discern individual photons with high temporal resolution. A simplified schematic for a SPAD detector is depicted in Figure 3, including the avalanche photodiode and the associated circuits responsible for active quenching, reset, and event readout. The SPADs operate in Geiger mode, where an avalanche of charge carriers, detectable as a current pulse, is triggered by an incoming photon. Several circuit factors can affect the performance of SPADs in pulsed ToF LIDAR systems, as outlined below:

- **Dead Time:** The detection of each photon prompts an avalanche event. Until this avalanche is quenched and the device reset, the SPAD remains incapable of detecting additional photons. This quench/reset time is known as dead time, a period of inactivity for the SPAD. This results in a temporal asymmetry, as initiating the avalanche is faster than quenching and restting. Consequently, dead time can lead to a loss of photons and a decreased dynamic range, especially under high-flux conditions.
- **Fill Factor:** Defined as the ratio of the SPAD's active sensing area to the total circuit area, the fill factor is typically reduced by the circuitry within the pixel, including quench and reset circuits. This reduction, in turn, decreases the detector's overall sensitivity. While higher fill factors are generally favored, they may also elevate the risk of crosstalk.
- **Dark Count Rate:** This refers to the frequency at which a SPAD triggers an avalanche in the absence of an incident photon. The dark count rate occurs due to the incident photons and thermally generated carriers in the diode's breakdown region. Higher dark count rates can amplify the background noise in depth measurements.
- **Background Illumination Rate:** This metric denotes the incident flux of photons unrelated to the pulsed ToF LIDAR system's illumination, such as sunlight or other artificial light sources, are detected. This rate can increase noise and reduce SNR in depth measurements.
- **Atmospheric Transmission:** As portrayed in Figure 1, the LIDAR signal travels from the source to the detector through the atmosphere. This journey can weaken the signal due to the atmosphere's absorption and scattering of the emitted light. This attenuation can affect the system's overall sensitivity, especially at greater distances.
- **Afterpulsing:** This phenomenon, where one photon detection event triggers subsequent detections, can also impact system performance. The present study did not consider this factor, focusing instead on situations with long dead times where after-pulsing effects will be less significant.

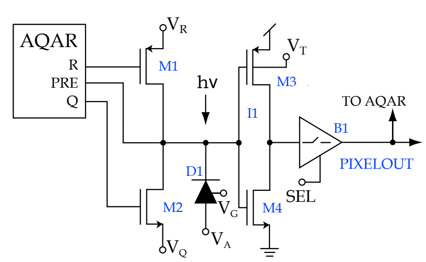

Fig. 3: Simplified Schematic of SPAD Pixel Circuit

IV. Simulation Study

We conducted a simulation study to explore the impact of various factors on the performance of SPAD-based pulsed ToF LIDAR systems. The study models key system components and their interactions using a custom simulation framework in Python. It considers the SPAD circuit considerations outlined

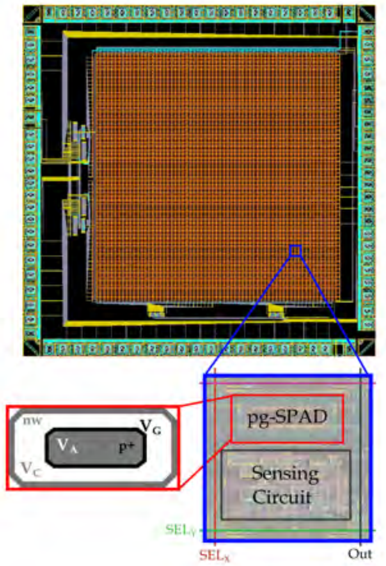

Fig. 4: Layout View of examplar SPAD array [7] where SEL_x is the column select line and SEL_y is the row select line

in Section III and models light propagation, photon detection, and depth estimation processes. We used Monte Carlo sampling techniques to incorporate the stochastic nature of photon arrivals and detection events [8]. We ran numerous simulations to gather statistically meaningful results. We based our parameter estimation and models for the SPAD array on values from [9]. The simulation includes the following assumptions, variables and parameters:

- **Number of SPADs (N) in the detector array:** We assume that the total area of the detector array is fixed at $0.1236\,\text{cm}^2$ and that this area can be allocated as a single SPAD or an array of SPADs with separate avalanche detection regions. In this work, the number of SPADs in the detector array varies from 1×1 to 64×64. Given a fixed area required for the in-pixel circuitry determined from the SPAD array in [9], the number of SPADs thus sets the pixel area, fill factor (as depicted in Figure 6), and incident photon count for a given light intensity.
- **Fill factor (FF):** We use a simple model shown in Figure 6 reflecting how the fill factor varies with pixel size. The model assumes a fixed area devoted to in-pixel circuits, with the remainder allocated to the sensor area. Larger sensors have a higher fill factor.
- **Number of emitted photons per pulse (E):** We vary the intensity of the transmitted light from 1000 to 10000 photons/sec.
- **Pulse width and repetition rate:** We vary the pulse width from 1e-8 to 1e-10 s and the repetition period from 1e-3 to 1e-4 second.
- **Reflectivity of the scene:** We have used reflectivity values ranging from 0.15 to 0.99 from the Middlebury2006 Dataset [10], [11].
- **Detector dead time (DDT) and dark count rate (DCR):** We assume a fixed dead time of 1e-9 s. Thermally generated carriers are assumed to follow a Poisson distribution, with the density of dark counts scaling with sensor area.
- **Atmospheric transmission(AT) and background illumination(BI):** We assume a fixed atmospheric transmission factor of 1.0 and background illumination of 100 photons/sec impinging on the array.

The optical components in our simulation define the raster scanning Field of View (FoV) to match the SPAD array's area. This setup allows for modeling different SPAD array sizes (1x1m through NxN), influencing the system's coverage and resolution. With a fixed sensor area and illumination, increasing the number of SPADs reduces the incident signal and increases the noise per SPAD. This is due to the light being distributed across more detectors and each SPAD contributing noise (mostly from dark counts). Thus, while larger SPAD arrays can potentially improve LIDAR spatial resolution, there is an associated tradeoff due to reduced signal and increased noise. Balancing these factors is an important consideration in SPAD-based LIDAR systems.

V. Results and Discussion

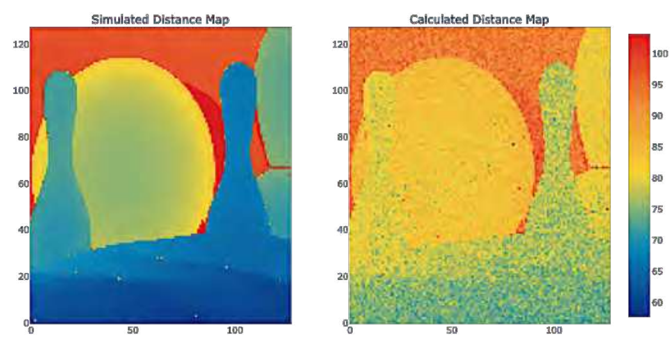

Fig. 5: Simulation Study: Comparison of Simulated Middlebury2006 Bowling Scene [10], [11] and Detected/Estimated Scene Depths

In this simulation study, the depth resolution of a pulsed LIDAR system is explored concerning the number of SPADs (single-photon avalanche diodes) incorporated into the array. The fill factor and dead time are critical considerations in this study. We model the dark count and background photons using Poisson-based interarrival times to simulate photon statistics. Simulation results reveal that the SPAD array configuration and the aforementioned factors strongly influence the performance of the pulsed LIDAR system. We utilized the bowling scene from Middlebury2006 [10], [11] to evaluate the accuracy of our simulation study, as shown in Figure 5. Raster scanning is employed for depth estimation, with the number of SPADs in the array determining the field of view. Reflected photons from the scene are generated according to pixel reflectivity and time of flight based on pixel depth values. The photons are simulated as Poisson events. To account for the dead time effect, we model the SPAD as unable to detect new photons during the dead time. We have also considered the

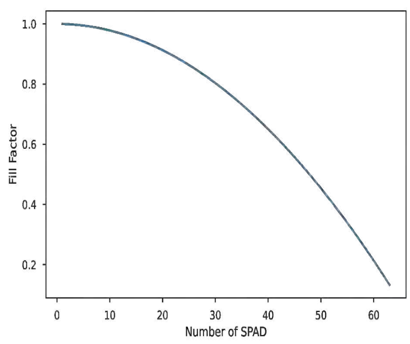

Fig. 6: Trade-off between fill factor for single SPAD and array configurations.

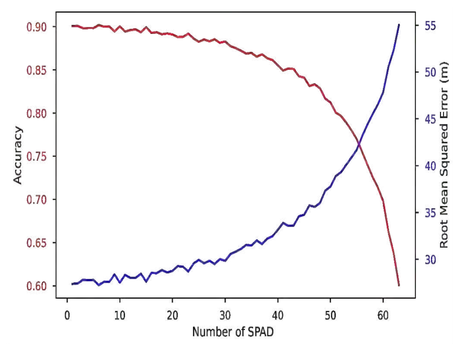

Fig. 7: Depth Resolution

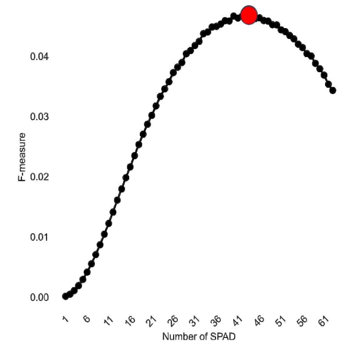

Fig. 8: Trade-off between depth accuracy and time resolution

quantum efficiency of the SPAD, which influences the number of photons detected by the sensor and, consequently, the overall performance of the depth estimation in the LIDAR system. The depth is estimated by determining the peak time of detected photons within the histogram, which represents the time of flight for the emitted light pulse to reach the target and return to the detector. The peak time is linearly related to the the distance to the target according to Eqn. (1). This simulation does not consider any limitations due to signal processing or readout, assuming that all events are detectable (except for those arriving during the detector dead time as discussed above).

We find that increasing the number of SPADs in an array decreases the depth resolution accuracy compared to single SPAD configurations, as depicted in Figure 7. The accuracy of the depth estimation can be quantified by comparing the simulated depth values with the actual depth values. Accuracy can be defined as:

$$Accuracy = \frac{\sqrt{\frac{1}{n}\sum_{i=1}^{n}(P_i - O_i)^2}}{O_{max} - O_{min}} \tag{2}$$

where P_i represents the predicted depth values, O_i represents the observed (actual) depth values, and n is the number of depth values compared. While in this simulation single SPADs offer better depth resolution due to their higher fill factor, this comes at the expense of increased time required for raster scanning in order to obtain an image of the scene.

The total time spent to obtain as image scales as:

$$O\left(\frac{P^2}{N^2}\right) \tag{3}$$

where P is the number of pixels in the scene and N is the number of SPADs in the array. The time is inversely proportional to the square of the number of SPADs since it is in terms of P/N squared. To determine the ideal number of SPADs in the array, we employ the F-measure to explore the tradeoff between the accuracy of depth resolution and imaging time in SPAD-based LIDAR systems.

$$F\text{-}measure = \frac{2 \times \text{Accuracy} \times \text{Total Time Spent}}{\text{Accuracy} + \text{Total Time Spent}} \tag{4}$$

When the number of SPADs is less than this optimal number, the reduction in depth accuracy dominates, causing a decrease in the F-measure. Conversely, when the number of SPADs exceeds the optimal number, the increase in time complexity outweighs the gains in depth accuracy, leading to a decrease in the F-measure.

This finding suggests that for a SPAD array of fixed total sensor area, there exists an optimal number of SPADs that offers the best balance between depth accuracy and imaging time, which, in the case of our simulation study, is approximately 40 as seen in Figure 8.

This simulation study provides insight into the performance of SPAD-based pulsed ToF LIDAR systems under various conditions. The results highlight the importance of optimizing SPAD array design to achieve accurate depth measurements and minimize the impact of noise and other unwanted effects.

VI. Conclusion

This paper has presented a commnuication channel model for pulsed ToF LIDAR-based depth imaging, emphasizing the role of SPAD circuit considerations in precise depth estimation. Through simulation, we have examined the influences of various factors on the operation of SPAD-based LIDAR systems, underscoring the necessity to optimize SPAD array configurations for superior depth imaging performance.

References

[1] J. Rapp, J. Tachella, Y. Altmann, S. McLaughlin, and V. K. Goyal, "Advances in Single-Photon LiDAR for Autonomous Vehicles: Working Principles, Challenges, and Recent Advances," *IEEE Signal Processing Magazine*, vol. 37, no. 4, pp. 62–71, Jul. 2020. [Online]. Available: https://ieeexplore.ieee.org/document/9127841/

[2] S. Scholes, G. Mora-Martín, F. Zhu, I. Gyongy, P. Soan, and J. Leach, "Fundamental limits to depth imaging with single-photon detector array sensors," *Scientific Reports*, vol. 13, no. 1, p. 176, Jan. 2023. [Online]. Available: https://www.nature.com/articles/s41598-022-27012-1

[3] B. Behroozpour, P. A. M. Sandborn, M. C. Wu, and B. E. Boser, "LiDAR System Architectures and Circuits," *IEEE Communications Magazine*, vol. 55, no. 10, pp. 135–142, Oct. 2017. [Online]. Available: http://ieeexplore.ieee.org/document/8067701/

[4] Y. Li and J. Ibanez-Guzman, "LiDAR for Autonomous Driving: The Principles, Challenges, and Trends for Automotive Lidar and Perception Systems," *IEEE Signal Processing Magazine*, vol. 37, no. 4, pp. 50–61, Jul. 2020. [Online]. Available: https://ieeexplore.ieee.org/document/9127855/

[5] F. Villa, F. Severini, F. Madonini, and F. Zappa, “SPADs and SiPMs Arrays for Long-Range High-Speed Light Detection and Ranging (LiDAR),” *Sensors*, vol. 21, no. 11, p. 3839, Jun. 2021. [Online]. Available: https://www.mdpi.com/1424-8220/21/11/3839

[6] ——. [Online]. Available: https://www.researchgate.net/figure/TOF-LiDAR-illumination-schemes-a-2D-raster-scan-with-single-spot-and-one-pixel_fig3_352060245

[7] M. S. R. Sajal and M. Dandin, “Concealable physically unclonable functions and key generation using a Geiger mode imager,” in *Proceedings of 2023 IEEE International Symposium on Circuits and Systems (ISCAS)*, Monterey, CA, USA, 2023, p. in press.

[8] V. Poisson, V. T. Nguyen, W. Guicquero, and G. Sicard, “Luminance-Depth Reconstruction From Compressed Time-of-Flight Histograms,” *IEEE Transactions on Computational Imaging*, vol. 8, pp. 148–161, 2022. [Online]. Available: https://ieeexplore.ieee.org/document/9706248/

[9] M. S. Sajal, K.-C. Lin, B. Senevirathna, S. Lu, and M. Dandin, “Perimeter-gated single-photon avalanche diode imager with vanishing room temperature dark count probability,” in *Proceedings of 2022 29th IEEE International Conference on Electronics, Circuits and Systems (ICECS)*, Glasgow, United Kingdom, 2022, pp. 1–4. [Online]. Available: https://ieeexplore.ieee.org/document/9970824

[10] D. Scharstein and C. Pal., “Learning conditional random fields for stereo,” *IEEE Computer Society Conference on Computer Vision and Pattern Recognition (CVPR 2007)*, 2007. [Online]. Available: http://www.cs.middlebury.edu/~schar/papers/LearnCRFstereo_cvpr07.pdf

[11] H. Hirschmüller and D. Scharstein., “Evaluation of cost functions for stereo matching,” *In IEEE Computer Society Conference on Computer Vision and Pattern Recognition (CVPR 2007)*, 2007. [Online]. Available: https://www.mdpi.com/1424-8220/21/11/3839